Available online at www.sciencedirect.com

SciVerse ScienceDirect

Ceramics International 38 (2012) 1417–1425

CERAMICS INTERNATIONAL

www.elsevier.com/locate/ceramint

$CaCO_3$ addition effect on the hydration and mechanical strength evolution of calcium aluminate cement for endodontic applications

A.P. Luz *, V.C. Pandolfelli

Federal University of São Carlos – Materials Engineering Department, Rod. Washington Luiz, km 235, São Carlos – SP, C.P. 676, CEP 13565-905, Brazil

Received 15 August 2011; received in revised form 7 September 2011; accepted 8 September 2011
Available online 14 September 2011

Abstract

Calcium aluminate cement (CAC) hydrates conversion can be inhibited by adding $CaCO_3$, leading to $C_3A{\cdot}CaCO_3{\cdot}11H$ ($3CaO{\cdot}Al_2O_3{\cdot}CaCO_3{\cdot}11H_2O$) formation. However, despite its benefits, the stability of this monocarbonate hydrate is not fully understood, especially when the samples are kept in contact with liquid during the curing step. Thus, taking into account the increasing interest in the CAC application as a biomaterial in the endodontic area, this work addresses the evaluation of the mechanical strength and phase transformations of a commercial cement (Secar 71) containing 15 or 20 wt% of $CaCO_3$. Compressive strength, apparent porosity, dimensional linear changes, X ray diffraction and thermogravimetric tests were carried out to evaluate samples immersed in water and kept at 37 °C between 1 and 30 days of curing. According to the collected results, CAH_{10} and C_2AH_8 formation were inhibited in $CaCO_3$ containing compositions and the presence of the $C_3A.CaCO_3.11H$ phase led to a significant cement mechanical strength increase. Nevertheless, the partial decomposition of this monocarbonate hydrate was detected at 37 °C in the range of 1–7 days and the continuous hydration of CA and CA_2 also affected the compressive strength behavior of the evaluated samples.

Keywords: Calcium aluminate cement (CAC); Hydration; $CaCO_3$; Monocarbonate (C_4ACH_{11})

1. Introduction

Recently continuous effort has been carried out in order to develop materials that present suitable properties and fulfill all requirements related to endodontic treatments, such as biocompatibility, improved sealing ability, dimensional stability, easiness for preparation and application, reduced setting time, high uniaxial compressive strength (>30 MPa) and cost values close to similar products used in this area [1–3]. Additionally, there is also great interest in the expansion of calcium aluminate cement (CAC) application as a biomaterial.

Some work attested the application of CAC based products as root canal filling materials, highlighting their biocompatibility features due to the *in situ* apatite crystals formation at the tooth–material interface [1,4–6]. Besides their short setting time, high mechanical strength and excellent performance in corrosive acid environment, CAC samples also presented better abrasion resistance than Portland cement and lower pH values during hydration when applied for dental restoration [2,7]. Moreover, additional investigations concluded that this sort of cement can be used for bone defect repairing, as its composition and expansion coefficient are similar to the tooth and human bone [2,3]. Nevertheless, in order to use CAC for endodontic treatments, it is required that at 37 °C (body temperature) and in contact with body fluids (liquid phase comprised by inorganic salts, such as phosphates, chlorides, etc.) no cement hydrate conversion should take place and the mechanical strength of this material should not decrease over time, but rather increase or be kept constant.

Calcium aluminate cements develop higher mechanical strength than conventional Portland ones at the early stages of their hydration process. The CAC hydration mechanism comprises the anhydrous phase dissolution which is followed by the precipitation of the hydrates (Table 1) from a saturated solution [8]. After these chemical transformations, the hydrates growth induces an interlocking effect and the formation of new bonds among these crystals, providing an increase in the cement mechanical strength [8–10].

* Corresponding author. Tel.: +55 16 33518253; fax: +55 16 33615404.
E-mail address: anapaula.light@gmail.com (A.P. Luz).

0272-8842/$36.00
doi:10.1016/j.ceramint.2011.09.021

Table 1
Properties of the main hydrates that can be formed in the calcium aluminate cement structure [10].

Phases	Chemical composition (wt%)			Temperature (°C)	Crystalline structure	Density (g/cm^3)
	CaO	Al_2O_3	H_2O			
CAH_{10}	16.6	30.1	53.5	<20	Hexagonal	1.72
C_2AH_8	31.3	28.4	40.3	20–30	Hexagonal	1.95
C_3AH_6	44.4	27.0	28.6	>30	Cubic	2.52
AH_3	–	65.4	34.6	>30	Hexagonal	2.42

C: CaO, A: Al_2O_3, H: H_2O.

AH_3 ($Al_2O_3{\cdot}3H_2O$ or $2Al(OH)_3$) and C_3AH_6 ($3CaO{\cdot}Al_2O_3{\cdot}6H_2O$) are the only CAC stable phases at 37 °C. Therefore, its mechanical strength can be affected by the CAH_{10} ($CaO{\cdot}Al_2O_3{\cdot}10H_2O$) and C_2AH_8 ($2CaO{\cdot}Al_2O_3{\cdot}8H_2O$) conversion reactions with the curing time and temperature (Fig. 1) [11–14]. The main drawback of the conversion process is related to the increase in the cement porosity (hydrates with lower density giving rise to denser ones, Table 1), resulting in a partial decrease of its mechanical properties. Hence, in order to attain a better performance of the calcium aluminate cements and inhibit these changes in their properties, these conversion reactions of the metastable hydrates should be avoided.

Some authors [11–13] have analyzed the effect of calcium carbonate additions on CAC compositions aiming to counteract the conversion process by the formation of a lamellar hydrate $C_3A{\cdot}CaCO_3{\cdot}11H$ also known as monocarbonate or calcium carboaluminate (C_4ACH_{11}). Its crystal structure is based on distorted main $[Ca_2Al(OH)_6]^+$ layers containing $[0.5CO_3{\cdot}2.5H_2O]^-$ ones inserted between them [12,13]. Another important aspect of the monocarbonate formation is its increasing effect on the cement hydration rate, resulting in a shorter material setting time [12].

Darweesh [11] stated that the partial CAC replacement by $CaCO_3$ should be up to 15 wt%, as higher contents can have a negative impact on the compressive strength of the cement compositions due to the lower amount of the main hydration products able to induce the bonding properties. On the other hand, some work has pointed out that depending on the curing conditions, the carbo-aluminous cement ($CaCO_3$ + CAC) will not be free from conversion type reactions, showing no clear agreement related to the stability and temperature of the $C_3A{\cdot}CaCO_3{\cdot}11H$ decomposition [12,13,15]. For example, some authors stated that the monocarbonate thermal decomposition may be carried out above 40 °C [15], whereas others also suggested that this hydrate becomes instable at 90 ± 5 °C [12].

Therefore, this work addresses the investigation of the mechanical properties and phase evolution of a commercial calcium aluminate cement (Secar 71) containing $CaCO_3$ samples cured at 37 °C and in contact with distilled water aiming at endodontic applications. The collected samples were evaluated by compressive strength, apparent porosity, dimensional linear change, X ray diffraction (XRD) and thermogravimetric (TG) tests. The $C_3A{\cdot}CaCO_3{\cdot}11H$ content was measured as a function of time in order to evaluate the stability of this phase and whether the hydrates conversion reactions could be identified in the range of 1–30 days of curing.

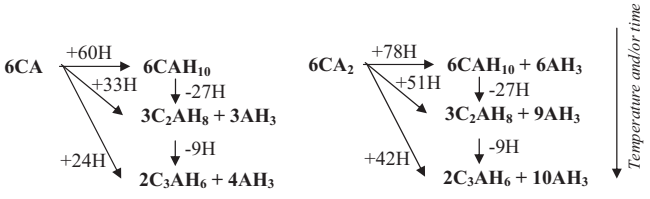

Fig. 1. General sketch representing the hydrate generation reactions for the calcium aluminate cement [14].

2. Experimental

Secar 71 cement (Kerneos, France – Table 2), calcium carbonate PA (Labsynth, $CaCO_3$, PA) and a polyethylene glycol based dispersant (Basf, Germany, recommended for calcium aluminate cement with high alumina content) were chosen for this study. The evaluated compositions and the raw material particle size distributions are presented in Table 3 and Fig. 2, respectively.

The cement pastes were prepared using 0.3 water/cement ratio (W/C). After the mixing step, cylindrical samples (diameter = 11 mm and height = 22 mm) were cast under vibration and kept in a moisture-saturated environment (∼100% RH) for 20 h at 37 °C ± 1 °C (Nova Ética equipment, model 403/D). After that, the samples were demolded, immersed in distilled water (pH = 7.1) and cured at 37 °C ± 1 °C. Due to the complexity of the CAC hydration process, the authors chose to firstly evaluate the cement behavior in contact with water in order to focus on the phase transformations derived from the $CaCO_3$ addition. Nevertheless, according to previous work [16], some changes in the amount of the hydrates in CAC samples were observed when in the presence of simulated body fluids (SBF), which can affect their mechanical properties due to the setting delaying effect induced by some of the ions contained in the solution.

After a curing period of 1, 3, 7, 15 and 30 days, five hydrated cement samples of each composition were tested for compressive strength (based on the ISO 9917-1 procedure)

Table 2
Chemical composition of the Secar 71 analyzed.

Chemical composition	Amount (wt%)
$CaAl_2O_4$ (or CA)	56.4
$CaAl_4O_7$ (or CA_2)	39.2
Al_2O_3	1.9
$Ca_{12}Al_{14}O_{33}$ (or $C_{12}A_7$)	2.1

Table 3
Cement compositions evaluated in this work.

Compositions	Secar 71 (wt%)	$CaCO_3$ (wt%)	Dispersant (wt%)
S	100	–	–
S-15C	85	15	0
S-20C	80	20	0
S-15C-D	85	15	0.6
S-20C-D	80	20	0.6

in MTS equipment (MTS Systems, Model 810, USA) using a strain rate of 0.5 mm/min and load cell of 50 kN. Moreover, the percentual dimensional linear change of the evaluated materials was determined as a function of the curing time, considering the initial and final height (before and after the curing step) divided by the initial sample height.

The cement samples attained after the mechanical strength tests were ground and microwave dried (Brastemp, model BMS25) for 6 min, using the highest power of this equipment – 700 W. As previously determined, this was a suitable procedure to allow the fully free water withdrawal of the cement samples resulting in a constant mass value for the evaluated materials [17].

After stopping the cement hydration, the collected samples were ground again (dp $<$ 45 μm) in a tungsten carbide mill (AMEF, model AMP1-M, Brazil) and analyzed using the X ray diffraction technique (Bruker equipment, model D8 Focus, Germany, with CuKα radiation [λ = 15,418 Å] and nickel filter, using 40 mA, 40 mV, scanning step = 0.02 for 2θ between 4° and 80°). The Rietveld method (Topas 4.2 software, Bruker) was used to analyze the XRD results in order to evaluate the amount of the hydrate phases comprising the collected samples for the chosen curing periods. Due to the lack of information in the literature about the symmetry and structure of the CAH_{10} and C_2AH_8 phases, a semi-quantitative evaluation of these hydrates (EVA software, Bruker) was carried out based on the calculation of the relative area of their most intense peaks.

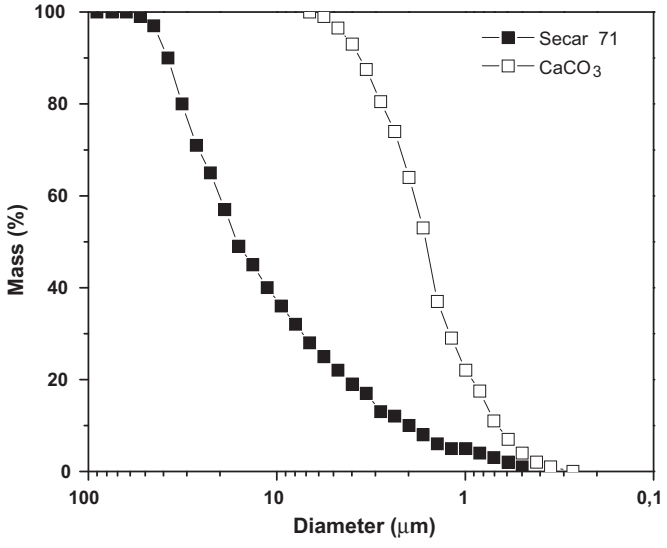

Fig. 2. Secar 71 and calcium carbonate particle size distributions.

TG evaluations were also carried out in NETZSCH STA 449 equipment, using a heating rate of 10 °C/min with a synthetic air (80% N_2–20% O_2) flow of 50 cm^3/min and α-Al_2O_3 as a correction standard. Due to the overlap of the $Al(OH)_3$ and C_3AH_6 hydrates decomposition peaks, a mathematical fitting analysis of the DTG curves was conducted using the Peak Analyzer module of the Origin® software (version 8.5.1 SR2) in order to calculate the amount of each phase contained in the cement samples. Additionally, the apparent porosity of the CAC samples (before halting the cement hydration) was measured by the Archimedes method (ASTM C380-00) using kerosene as immersion liquid.

3. Results and discussion

Adding 14 wt% of $CaCO_3$ to CAC compositions would result in the required amount of $C_3A{\cdot}CaCO_3{\cdot}11H$ to inhibit the CAH_{10} and C_2AH_8 hydrates formation and their further conversion (Fig. 1). However, as suggested by Kuzel et al. [12], the use of 15 or 20 wt% of this additive can reduce the metastable hydrates crystallization more effectively.

According to Fig. 3, the carbo-aluminous cement pastes presented a significant mechanical strength increase when

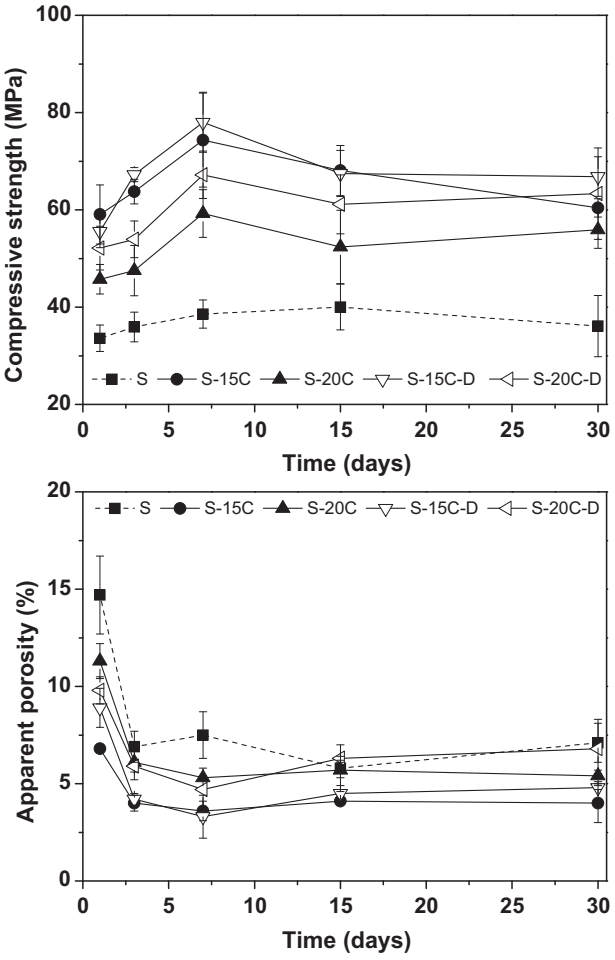

Fig. 3. Compressive strength and apparent porosity results for the cement samples kept immersed in distilled water at 37 °C (where S = Secar 71, C = $CaCO_3$ and D = dispersant).

compared to the S samples (plain Secar 71 cement), mainly for the 15 wt% $CaCO_3$ containing composition. This better performance could be related to the improved particle packing of these compositions, as the finer particles of this carbonate fill in the voids among the cement ones. Thus, in order to analyze this aspect, the particle size distribution of the studied materials was theoretically compared to the Alfred packing model ($q = 0.15$) [18] using the PSDesigner software (Alcoa–UFSCar, Brazil). The decrease in the quadratic deviations ($r^2 = 0.37180$, 0.06263 and 0.03848 for S, S-15C and S-20C, respectively) indicated that a better fitting to the target curve was attained when higher amounts of $CaCO_3$ were added to the Secar 71. Nevertheless, the evaluated samples containing 20 wt% of calcium carbonate did not present the highest compressive strength values and, therefore, other factors should also be affecting the cement performance.

The improved mechanical behavior of the dispersant containing compositions (S-15C-D and S-20C-D) might be associated to a better dispersion efficiency of their particles. As will be further discussed, this additive also has an important role in the hydration reaction steps, changing the amounts of the generated hydrate phases.

The increase in the compressive strength was followed by the decrease in the apparent porosity values in the range of 1–7 days for the evaluated materials (Fig. 3). This behavior is associated with the continuous hydrated phases formation and precipitation in the available pores [11]. However, this trend was not kept between 7 and 30 days, where a small drop of the

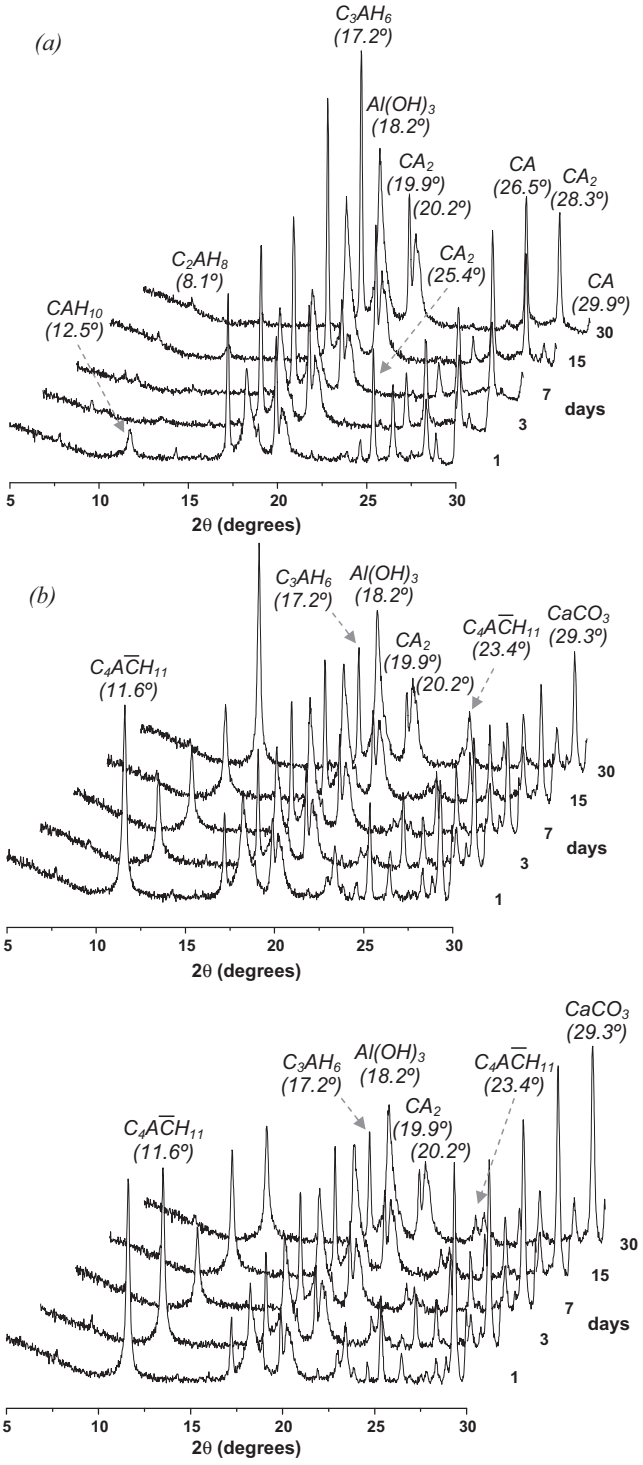

Fig. 4. XRD profiles for (a) S, (b) S-15C-D and (c) S-20C-D samples attained as a function of the curing time.

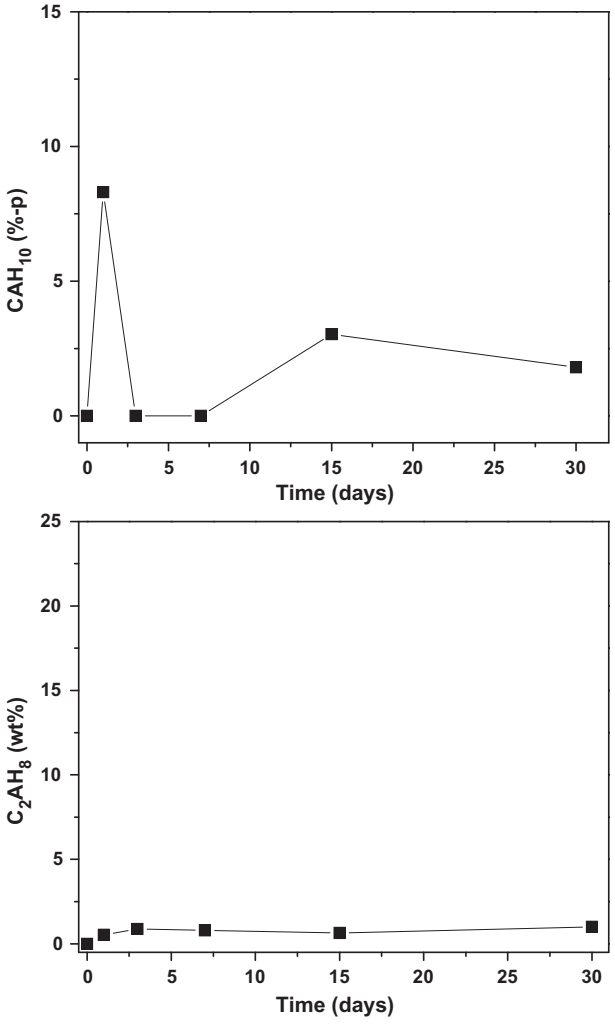

Fig. 5. Evolution of the CAH_{10} and C_2AH_8 hydrate contents for the Secar 71 cement (S) at 37 °C (average standard deviation was close to ±1% for all tested conditions).

mechanical strength and some changes in the sampleś porosity values were observed.

Aiming to understand the influence of the phase transformations on the cement properties, qualitative and quantitative analyses of the X ray diffraction results were carried out. Fig. 4 presents the XRD profiles for the S, S-15C and S-20C compositions.

The main identified hydrates in the S cement were C_3AH_6 and $Al(OH)_3$, but other phases such as CAH_{10} and C_2AH_8 were also present. CAH_{10} was only detected at the 1st, 15th and 30th day with contents close to 8.3 wt%, 3.0 wt% and 1.8 wt%, respectively (Fig. 5). Thus, the absence of this hydrate at the 3rd and 7th day can be related to its conversion, giving rise to the stable components C_3AH_6 and $Al(OH)_3$. The CAH_{10} formation at the 15th and 30th days should be due to the anhydrous phases hydration (CA and CA_2 contained in the S samples) or the high water amount in contact with the cement sample. In addition, small C_2AH_8 peaks were also identified in the XRD profile of the Secar 71 composition (Fig. 4a), attesting that the metastable hydrates formation can take place at 37 °C due to the high water availability in the curing environment and the sample size.

High contents of anhydrous phases were identified in the Secar 71 composition (Fig. 6a and b). Hence, the continuous CA and CA_2 hydration led to an expressive mechanical strength increase and the decrease of the apparent porosity values in the range of 1–7 days. For longer curing time (>15 days), the slight drop of the modulus of rupture followed by the increase in the S samples porosity can be associated to the balance between the consumption of the available anhydrous phases (CA and CA_2 contents are close to zero after 30 days, Fig. 6) and the CAH_{10} and C_2AH_8 conversion reactions to C_3AH_6 and $Al(OH)_3$ hydrates (Fig. 1).

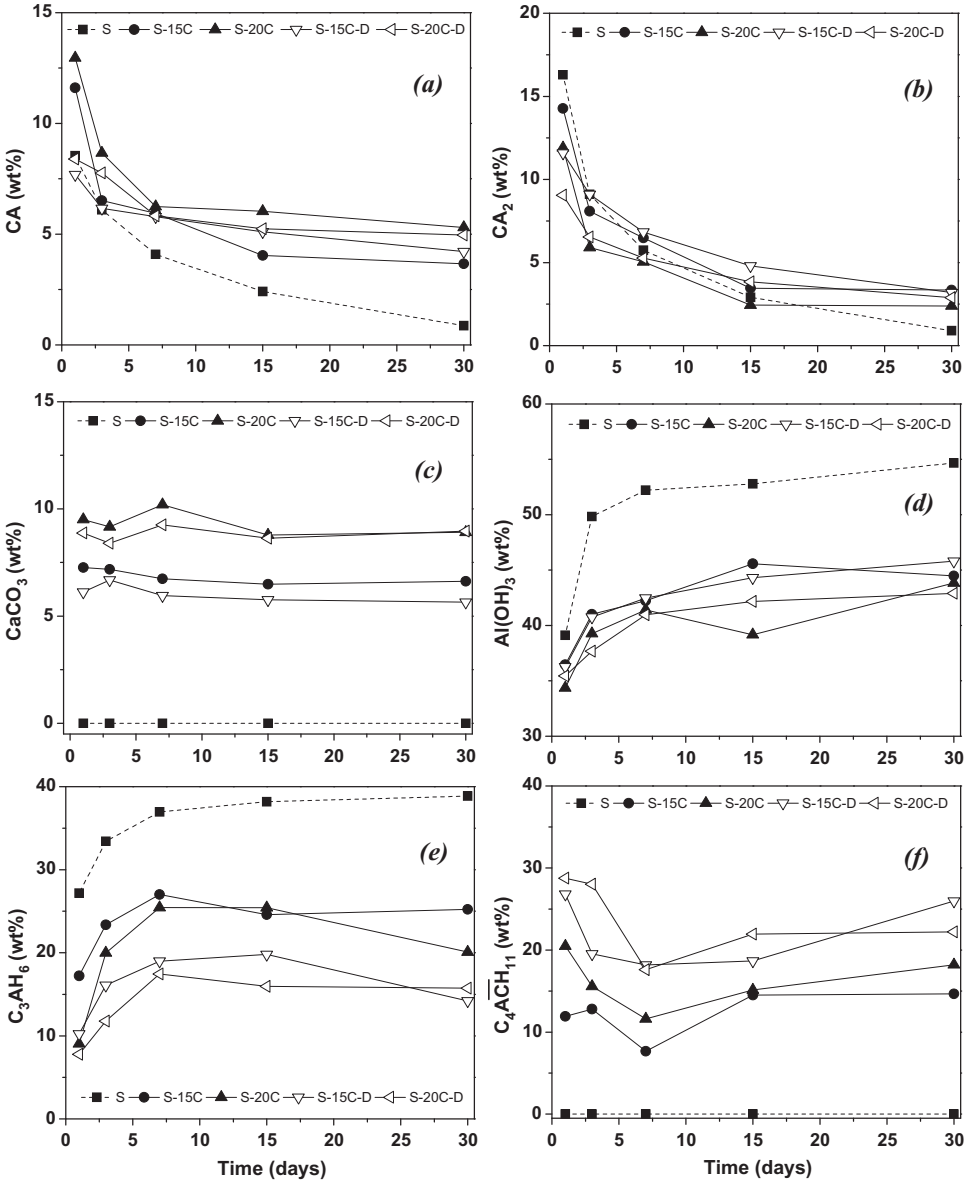

Fig. 6. Evolution of the phase contents for the evaluated cement compositions at 37 °C and as a function of time (average standard deviation was close to ±1% for all tested conditions).

Regarding the carbo-aluminous compositions, $C_3A{\cdot}CaCO_3{\cdot}11H$ (or C_4ACH_{11}) was quickly formed, and the main hydrate was found in the S-15C and S-20C samples on the first day of curing (Fig. 4b and c). The following equations describe this transformation [11]:

$$CaCO_3 + 3CA + 17H \rightarrow C_3A \cdot CaCO_3{\cdot}11H + 2AH_3 \quad (1)$$

$$CaCO_3 + 3CA_2 + 26H \rightarrow C_3A \cdot CaCO_3{\cdot}11H + 5AH_3 \quad (2)$$

CAH_{10} and C_2AH_8 were not detected in those cement samples, confirming that the monocarbonate presence inhibited their formation. Moreover, C_3AH_6 and $Al(OH)_3$ were identified in lower amounts than the ones found in S cement (Fig. 6d and e, which can be related to the reduced CAC content in the S-15C and S-20C compositions) and a further reaction between C_3AH_6 and $CaCO_3$ can also give rise to $C_3A{\cdot}CaCO_3{\cdot}11H$ crystals (Eq. (3)) [12].

$$CaCO_3 + C_3AH_6 + 5H \leftrightarrow C_3A \cdot CaCO_3{\cdot}11H \quad (3)$$

However, it must be highlighted that this is a reversible reaction and the monocarbonate decomposition can still take place depending on time, temperature and humidity. As presented before, some work stated that $C_3A{\cdot}CaCO_3{\cdot}11H$ thermal decomposition may occur in the temperature range of 40–90 °C [12,15]. Nevertheless, the decrease in this phase content was observed between 1 and 7 days for the evaluated conditions presented in this work (samples were cured at 37 °C and immersed in distilled water).

The $C_3A{\cdot}CaCO_3{\cdot}11H$ ($\rho = 2.17$ g cm^{-3}) decomposition results in the formation of denser phases (C_3AH_6 = 2.52 g cm^{-3} and $CaCO_3$ = 2.72 g cm^{-3}) and, therefore one could expect that the samples' porosity should increase throughout the 7 first days of curing. However, the opposite trend was detected in the experimental analyses and this behavior may be associated with the CA and CA_2 hydration and further precipitation of new hydrates (monocarbonate, C_3AH_6 and $Al(OH)_3$) in the formed pores. Additionally, an increase in the $CaCO_3$ content (Fig. 6c) should have been detected after the partial monocarbonate decomposition, which was not observed.

Although the $C_3A{\cdot}CaCO_3{\cdot}11H$ phase helps to provide higher mechanical strength to the cement samples on the first day of curing, its partial decomposition, added to the continuous hydration of the CA and CA_2 phases seem to be some of the key factors that led to a further improvement in the compressive results up to the 7th day. Further investigations are still required in order to better explain the balance effect in this complex system where a dynamic phase change is carried out on the first 7 days of curing.

After this period, additional CA and CA_2 hydration and $C_3A{\cdot}CaCO_3{\cdot}11H$ crystals formation (Fig. 6f), by consuming C_3AH_6 hydrate (Eq. (3)), are pointed out as the chemical transformations responsible for decreasing the mechanical behavior of the evaluated carbo-aluminous cement samples.

Another important aspect to be highlighted is the dispersant effect on the S-15C-D and S-20C-D cements phase evolution. After 1 day of curing, the higher hydration rate of the CA and CA_2 phases resulted mainly in the $C_3A{\cdot}CaCO_3{\cdot}11H$ generation for the dispersant containing samples (Fig. 6). Therefore, the presence of this additive sped up the CAC hydration process and Eqs. (1) and (2) would be the dominant ones. Some small changes among the CA, CA_2 and $Al(OH)_3$ contents in the cement samples with or without the polyethylene glycol based dispersant were also observed as a function of the time. In addition, the amount of C_3AH_6 phase attained in these compositions was lower than the one detected in the dispersant free cements.

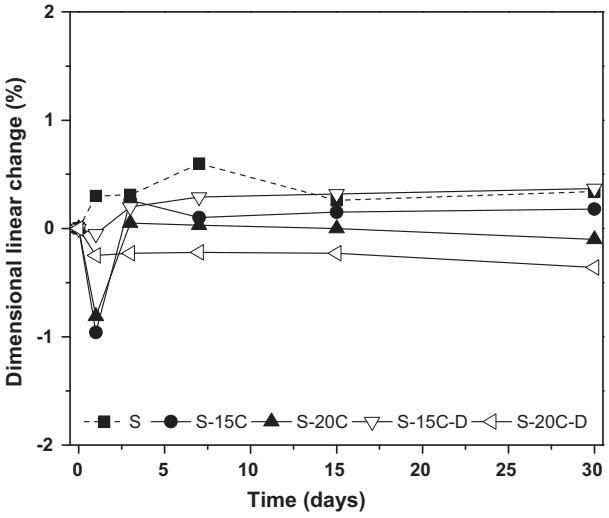

Fig. 7. Dimensional linear changes of the cement samples during the curing step.

As observed in Fig. 7, the use of a polymeric dispersant can affect the dimensional stability of the prepared samples. The phase transformations identified on the first day (mainly the monocarbonate formation) caused the shrinkage of the carbo-aluminous cement materials and this effect was more significant in the dispersant free compositions, which contained lower amounts of $C_3A{\cdot}CaCO_3{\cdot}11H$ ($\rho = 2.17$ g cm^{-3}). Conversely, the S samples showed an opposite trend (expansion) between 1 and 7 days and C_3AH_6 and $Al(OH)_3$ were the main phases generated.

The dimensional stability evaluation of the cement materials applied in the endodontic treatments has not been included in the ISO 6876:2001 standard procedures. However, there is a consensus among the users that these products should have expansion or shrinkage values lower than 1%. Some authors [19] pointed out that a controlled expansion can help to attain a suitable apical sealing, but an exceeded one would lead to microcracks and/or dental fracture. Based on the collected results (Fig. 5), all tested compositions fulfilled the requirements and in the presence of the polymeric dispersant the dimensional stability was even higher (S-15C-D and S-20C-D samples).

Due to a poor crystallinity of the products formed at early age hydration, the thermal analysis (DTA/TG) could help to identify some other phases present [20,21]. Some major changes in the DTA signal were observed during the heating step of the cement samples and, therefore, the DTG curves (as shown in Fig. 8) were chosen due to their straight baseline,

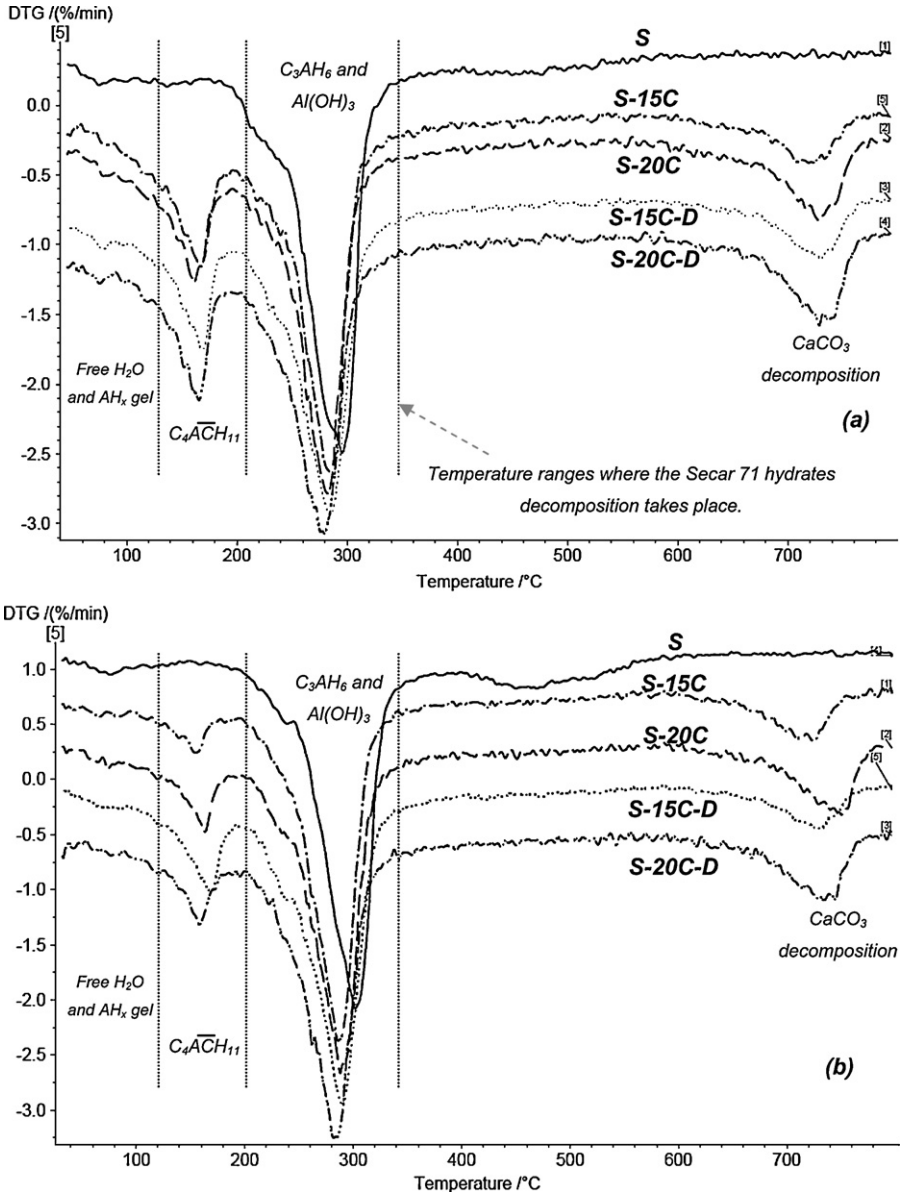

Fig. 8. DTG curves for the samples attained after (a) 1 and (b) 30 days of curing.

allowing a more precise identification of the hydrated phases according to their characteristic dehydration peaks.

Cement S presented an intense peak close to 298 °C indicating that C_3AH_6 and $Al(OH)_3$ should be the major containing phases in this material, as their decomposition is expected to take place at 300 °C and 285 °C, respectively [22]. The peaks of the $C_3A{\cdot}CaCO_3{\cdot}11H$ and $CaCO_3$ were identified between 161–169 °C and 728–730 °C, respectively, for the calcium carbonate containing compositions. Nevertheless, the overlap of the $Al(OH)_3$ and C_3AH_6 hydrates decomposition peaks makes a suitable quantitative evaluation of the attained results difficult. In order to determine the amount of each hydrated phases, a mathematical fitting analysis was carried out (Peak Analyzer, Origin® software) and the collected results are shown in Table 4. Additionally, Fig. 9 presents the S-20C-D (attained after 30 days of curing) DTG curve and the fitted peaks, indicating the good correlation between the chosen mathematical function (Lorentz) [23] and the experimental data.

According to the calculated areas (Table 4), there was a decrease in the monocarbonate peaks intensity with the advance of the curing time (which can also be observed in Fig. 4b and c), confirming that the decomposition of this hydrate took place in the evaluated experimental conditions proposed in this work (37 °C and in contact with water). As observed in the quantitative XRD data (Fig. 6), C_4ACH_{11} should be the main phase formed in the carbo-aluminous compositions containing a dispersant additive (S-15C-D and S-20C-D) after 1 day. In addition, the decomposition of this phase throughout the 30 days of curing was followed by further $CaCO_3$ formation, mainly for the samples containing 15 wt% of this carbonate (Table 4). A direct comparison of Table 4 and Fig. 6 results is not possible, as for the TG analysis the quantification of the CA and CA_2 phases present in the compositions could not be carried out.

Table 4
Peak area (%) and regression coefficient attained in the mathematical fitting analysis of the DTG curves.

Samples	Curing time (days)	Percentual peak area (%)				Regression coefficient (r^2)
		C_4ACH_{11}	$Al(OH)_3$	C_3AH_6	$CaCO_3$	
S	1	–	67.13	32.87	–	0.99
S-15C		30.71	35.72	23.51	10.07	0.99
S-20C		27.61	33.99	22.58	15.82	0.98
S-15C-D		31.77	30.91	26.24	11.07	0.98
S-20C-D		31.69	28.78	23.66	15.86	0.97
S	30	–	61.69	38.31	–	0.98
S-15C		11.57	39.22	32.79	16.42	0.99
S-20C		14.48	38.99	29.69	16.84	0.98
S-15C-D		19.07	32.62	33.21	15.10	0.99
S-20C-D		16.11	33.33	33.60	16.95	0.99

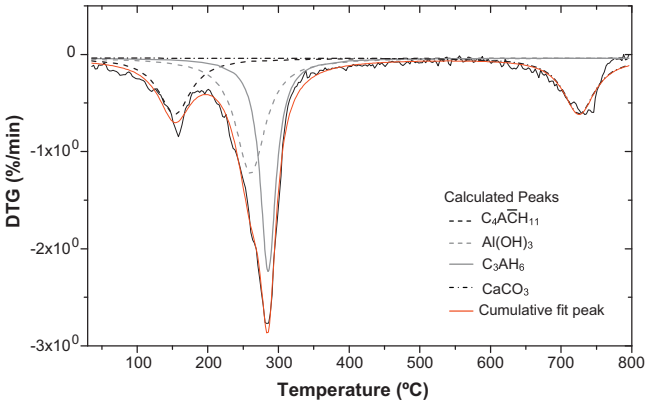

Fig. 9. Mathematical fitting analysis of the S-20C-D DTG curve (sample attained after 30 days of curing).

Samples S, S-15C and S-20C presented $Al(OH)_3$ as their main hydrate (peak with the highest area) and, over time, a clear increase in this hydroxide and C_3AH_6 contents was detected for the evaluated materials (except for plain Secar 71 cement). In general, the same chemical transformations detected by the quantitative XRD technique were observed in the mathematical fitting analysis by the DTG curves. Therefore, due to the good correlation attained from this method (regression coefficient close to 0.97–0.99), the Peak Analyzer module can be a suitable tool to be applied when evaluating the TG/DTG results for the calcium aluminate cement compositions, allowing a more accurate identification of the phase transformations attained during the curing step.

4. Conclusions

Adding $CaCO_3$ to calcium aluminate cement (Secar 71) induced the $C_3A{\cdot}CaCO_3{\cdot}11H$ hydrate formation in the evaluated curing conditions (37 °C with samples immersed in water between 1 and 30 days), inhibiting the formation/conversion of the CAH_{10} and C_2AH_8 metastable phases. Moreover, although the monocarbonate phase provides high mechanical strength to the cement samples on the first day of curing, its decomposition combined with the C_3AH_6 and $Al(OH)_3$ generation due to the continuous hydration of CA and CA_2 phases, seem to be some of the factors that led to a further improvement in the compressive results up to the 7th day. Further investigations are still required in order to explain the effect of each transformation on the cement properties throughout this dynamic phase change detected on the first 7 days of curing. In addition, as presented by some authors in the literature, this work attested the instability of the monocarbonate in temperatures close to 40 °C, instead of 90 °C predicted by others.

Another important aspect to be highlighted is the dispersant effect on the cement phase evolution, speeding up the anhydrous phase hydration, improving the samples dimensional stability and mechanical performance. Thus, despite the partial $C_3A{\cdot}CaCO_3{\cdot}11H$ decomposition, the calcium carbonate addition to CAC cements can be a good alternative to suppress the CAH_{10} and C_2AH_8 conversion reactions, leading to a better mechanical performance and dimensional stability in experimental conditions required in the endodontic treatments.

Acknowledgements

The authors are grateful to the Conselho Nacional de Desenvolvimento Científico e Tecnológico (CNPq) for supporting this work and Kerneos Inc. (France) for supplying the cement.

References

[1] M. Jacobovitz, M.E. Vianna, V.C. Pandolfelli, I.R. Oliveira, H.L. Rosseto, B.P.F.A. Gomes, Root canal filling with cements based on mineral aggregates: an in vitro analysis of bacterial microleakage, Oral Surg. Oral Med. Oral Pathol. Oral Radiol. Endodontol. 108 (2009) 140–144.
[2] J. Loof, Calcium-aluminate as biomaterial. Synthesis, design and evaluation [Dissertation]. Faculty of Science and Technology, Uppsala University (2008), 1–87.
[3] L. Kraft, Calcium aluminate based cement as dental restorative materials [Dissertation]. Faculty of Science and Technology, Uppsala University (2002), 1–65.
[4] V.C. Pandolfelli, I.R. Oliveira, M. Jacobovitz, H.L. Rosseto, Aluminous cement-based composition for application in endodontics and cementitious product obtained therof. Patent No. WO2009067774 (2009).
[5] H. Engqvist, J.E. Schultz-Walz, J. Loof, G.A. Botton, D. Mayer, M.W. Phaneuf, N.O. Ahnfelt, L. Hermansson, Chemical and biological

integration of a mouldable bioactive ceramic material capable of forming apatite in vivo in teeth, Biomaterials 25 (2004) 2781–2787.
[6] J. Loof, F. Svahn, T. Jarmar, H. Enqvist, C.H. Pameijer, A comparative study of the bioactivity of three materials for dental applications, Dental Mater. 24 (2008) 653–659.
[7] J. Loof, H. Engqvist, K. Lindqvist, N.O. Ahnfelt, L. Hermansoon, Mechanical properties of a dental restorative material based on calcium aluminate, J. Mater. Sci. Mater. Med. 14 (2003) 1–5.
[8] C. Parr, Calcium aluminate cement – what happens when things go wrong? in: Proceedings IRE annual conference, UK, (2008), pp. 1–11.
[9] I.R. Oliveira, V.C. Pandolfelli, Castable matrix additives and their role on hydraulic binder hydration, Ceram. Int. 35 (2009) 1453–1460.
[10] J.E. Kopanda, G. Maczura, Production Processes, Properties, and Applications for Calcium Aluminate Cements, 15212, Aluminum Company of America, Pittsburg, PA, 1987, 171–183.
[11] H.H.M. Darweesh, Limestone as an accelerator and filler in limestone-substituted alumina cement, Ceram. Int. 30 (2004) 145–150.
[12] H.J. Kuzel, H. Baier, Hydration of calcium aluminate cements in the presence of calcium carbonate, Euro. J. Miner. 8 (1996) 129–141.
[13] C.H. Fentiman, Hydration of carbo-aluminous cement at different temperatures, Cem. Concr. Res. 15 (1985) 622–630.
[14] P. Pena, A.H. De Aza, Cementos de aluminatos cálcicos. Constitución, características y aplicaciones, in: Refractarios Monolíticos, Soc. Esp. Cerám. Y Vidrio, 1999 85-106.
[15] G.P. Wojciech, The Effect of Limestone Fillers on Sulfate Resistance of High Alumina Cement Compositers. Calcium Aluminate Cements, E & FN Spon, London, 1990, 241-255.
[16] A.P. Luz, N.Z. Borba, V.C. Pandolfelli, Mechanical strength and hydrate products evolution of calcium aluminate cement for endodontic applications. Ceramica, Brazil (in Portuguese), in press.
[17] A.P. Luz, V.C. Pandolfelli, Halting the calcium aluminate cement hydration process. Ceram. Int., in press. DOI 10.1016/j.ceramint.2011.06.034.
[18] R.G. Pileggi, A.R. Studart, M.D.M. Innocentini, V.C. Pandolfelli, High performance refractory castables, Am. Ceram. Soc. Bull. 81 (2002) 37–42.
[19] M. Torabinejad, T.F. Watson, T.R. Pitt, Ford sealing ability of a mineral trioxide aggregate when used as a root-end filling material, J. Endod. 19 (1993) 591–595.
[20] J. Dweck, P.M. Buchler, A.C.V. Coelho, F.K. Cartledge, Hydration of a Portland cement blended with calcium carbonate, Thermochim. Acta 346 (2000) 105–113.
[21] N. Ukrainczyk, T. Matusinovic, S. Kurajica, B. Zimmermann, J. Sipusic, Dehydration of a layered double hydroxide – C_2AH_8, Thermochim. Acta 464 (2007) 7–15.
[22] V.S. Ramachandran, Applications of Differential Thermal Analysis in Cement Chemistry, Chemical Publishing Company, New York, 1969, 206–212.
[23] S.C. Arora, G. Datt, S. Verma, Operators on Lorentz sequence spaces, Math. Bohemica 134 (1) (2009) 87–98.